ACTA METALLURGICA SINICA (ENGLISH LETTERS)
Vol. 17 No. 3 pp 229-237 June 2004

A 2-D FINITE ELEMENT MODEL SIMULATION OF THE MELTING PROCESS OF Al-Ti ALLOY IN VACUUM INDUCTION FURNACE WITH COLD CRUCIBLE (VIFCC)

S.C. Chu and S.S. Lian
Institute of Materials Science and Engineering, National Taiwan University, Taibei (Taipei)
F.K. Chen
Institute of Mechanical Engineering, National Taiwan University, Taibei (Taipei)
Manuscript received 11 October 2003

The development of a numerical model for the melting process of Al-Ti alloy target material in vacuum induction furnace with cold crucible (VIFCC) was described. It is a two-dimensional computational methodology to calculate electromagnetic field, heat transfer field and fluid flow field . Based on the aid of the finite element method with the commercial software—ANSYS, a superimposition method of a layer of copper and a slit to simulate the VIFCC melting process was used. The method was effective to save large quantity of memory and computing time. Meanwhile, a temperature distribution profile during the melting process was obtained. Validity of the model was confirmed by comparison between the result from calculation and those from direct measurement by optical pyrometer and indirect investigation by ingot macrostructure. A relatively good agreement was found. Further, a nearly directional solidification structure was obtained under properly controlling the cooling rate and heating power. Therefore, such model developed in this article is feasible.
KEY WORDS *VIFCC, ANSYS, superimposition, ingot macrostructure*

1. Introduction

Recently, target materials have received great interests due to the fast growing of computer and semiconductor industries. Hence the demand for high purity metals or clean alloys, such as Al-Ti alloys, has increased greatly. The target materials require not only cleanness and few inclusions but also good microstructure, which imply that it should have small grain size, less pores and homogenous compositions. Vacuum induction furnace with water-cooled copper-crucible (VIFCC) has recently received considerable attention for the melting of reactive metals because its cost is lower than electron beam melting (EBM) and vacuum arc melting (VAM), and a fare quality of the melted alloys will be obtained. In addition VIFCC can eliminate the reactions between the melt of the alloys and the refractory of the crucible in vacuum induction melting (VIM) due to a unique feature of the VIFCC melting process possessing, in which the liquid metal is kept in a solid skull of the same metal without contacting the crucible, and is stirred by the electromagnetic force[1−3]. The processes can also have a control of alloy solidification with its water-cooled crucible. However, the VIFCC melting furnace has the disadvantages of low melting efficiency and a high temperature gradient that will probably cause inhomogeneity in the melt of alloys in a larger furnace. In order to obtain the best quality ingot with a limited melting power, the temperature distribution of the melt and its relationship with the melting parameters

need to be known. It is therefore the object of this study to simulate the temperature distributions of the melts of Al-Ti alloys in VIFCC with finite element technique.

The modeling of VIFCC is more complex than induction melting with refractory crucible, because factors such as geometry, dimension of the crucible, segment number, slot, coil design, induction frequency are all important to the melting efficiency. Although simulation of induction melting has been reported in previous studies which include the eddy current distribution in a cold crucible[4] or the free surface shape in the molten metal[5], few works have been done in temperature distribution. In order to have a better experimental design to improve the ingot quality, we have developed a 2D model simulation with integration of a harmonic electromagnetic and transient thermal phenomena analysis in this paper. The results of modeling are verified with the measured temperatures and the macrostructure of the ingot.

2. Description of the Modeling

In this model, the copper crucible and the Al-Ti alloy are located inside the coils. The alternating current that passes through the coils creates an alternating magnetic field. The load (copper crucible and alloy) placed within this field becomes part of the electromagnetic circuit. Heat will then be generated inside the alloy due to the induced eddy current. Since the induction-heating provides a nearly uniform heat flux to the alloy, this model shall assume that the system is axisymmetric. A geometric model of VIFCC with axisymmetric cylinder system, which is equipped with the water-cooled copper crucible, is shown in Fig.1. This is a quarter of the model. The topside schematic representation is shown in Fig.2. The arrow shows the direction of current and an AC current is assumed to pass through the coil, then the copper crucible will induce an eddy current in the opposite direction. In the same way, the molten metal induces an eddy current in the opposite direction with the copper segments. The magnetic field direction is up through the paper.

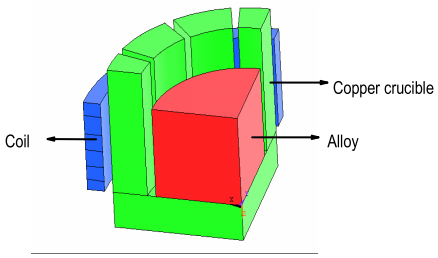

Fig.1 A geometric model of VIFCC with axisymmetric cylinder.

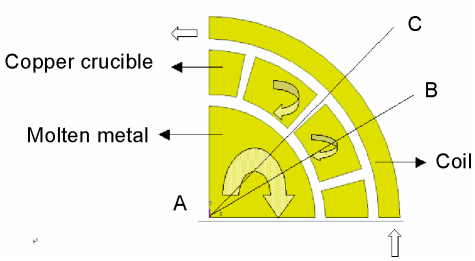

Fig.2 The topside schematic representation.

2.1 Theoretical formulation

A harmonic electromagnetic governing equation is formulated from Maxwell's equations, where $\boldsymbol{H}$ denotes the magnetic field intensity vector, $\boldsymbol{D}$ the electric flux density, $\boldsymbol{J}$ the total current density vector, $\boldsymbol{E}$ the electric field, $\boldsymbol{B}$ the magnetic field, σ the electric conductivity, and μ the magnetic permeability

$$\nabla \times \{\boldsymbol{H}\} = \{\boldsymbol{J}\} + \{\frac{\partial \boldsymbol{D}}{\partial t}\} = \{\boldsymbol{J}_{\mathrm{s}}\} + \{\boldsymbol{J}_{\mathrm{e}}\} + \{\frac{\partial \boldsymbol{D}}{\partial t}\},\ (\frac{\partial \boldsymbol{D}}{\partial t} = 0) \tag{1}$$

$$\nabla \times \{\boldsymbol{E}\} = -\{\frac{\partial \boldsymbol{B}}{\partial t}\} \tag{2}$$

$$\nabla \cdot \{\boldsymbol{B}\} = 0 \tag{3}$$

From constitutive equations

$$\{\boldsymbol{B}\} = [\mu]\{\boldsymbol{H}\} \tag{4}$$

$$\{\boldsymbol{J}\} = [\sigma]\{\boldsymbol{E}\} \tag{5}$$

Where μ and σ denote magnetic permeability and electrical conductivity, respectively.

Since it's a cylindrical coordinate system, the tangent system of the coordinates (r, θ, z) will be ($\vec{e}_\theta$, $\vec{e}_r$, $\vec{e}_z$). Therefore the current density is $j = j(r,z)e^{iwt}$, w is the angular frequency. From $\nabla \cdot \boldsymbol{B} = 0$, we can define a vector potential $\boldsymbol{A}$[6].

$$\boldsymbol{B} = \nabla \times \boldsymbol{A} \tag{6}$$

Where $\boldsymbol{A} = e^{iwt}\phi(r,z)\vec{e}_\theta$.

Using Eq.(6), and substituting $\boldsymbol{B}$ into Eq.(5), $\boldsymbol{H}$ is got. In a similar way, substituting $\boldsymbol{H}$ into Eq.(1), the electromagnetic governing equation becomes

$$\frac{\partial}{\partial r}(\frac{1}{\mu r}\frac{\partial(r\phi)}{\partial r}) + \frac{\partial}{\partial z}(\frac{1}{\mu}\frac{\partial(\phi)}{\partial z}) = \boldsymbol{J} = \boldsymbol{J}_{\mathrm{s}} + \boldsymbol{J}_{\mathrm{e}} \tag{7}$$

Here $\boldsymbol{J}_{\mathrm{s}}$ is the applied source current density and $\boldsymbol{J}_{\mathrm{e}}$ is the induced eddy current density vector. For the axisymmetric cylindrical coordinate system, the heat transfer equation is governed by[7]

$$\frac{1}{r}\frac{\partial}{\partial r}(kr\frac{\partial T}{\partial r}) + \frac{\partial}{\partial z}(k\frac{\partial T}{\partial z}) + q_{\mathrm{g}} - q_{\mathrm{out}} = \rho c_p \frac{\partial T}{\partial t} \tag{8}$$

Using the following equation combine electromagnetic and heat transfer field

$$q = \frac{\boldsymbol{J}_{\mathrm{e}}^2}{\sigma} = \frac{(\sigma\frac{\partial \boldsymbol{A}}{\partial t})^2}{\sigma} = \sigma(\frac{\partial \boldsymbol{A}}{\partial t})^2 = \sigma(\frac{\partial(e^{iwt}\phi(r,z)\vec{e}_\theta)}{\partial t})^2 \tag{9}$$

2.2 The finite element model

In order to find the temperature distribution of the molten metal, a simple and fast 2D model is used. If it is assumed that a quasi-steady state is established, there exists a steady molten metal with negligible shape change, which does not change with time. The model assumes that the system has reached a steady state. Further, the fluid flow and the velocity field in the system can be shown to be negligible.

The thermal analysis of cold crucible in induction melting is actually 3-D modeling problem. However, the computer simulation of 3-D modeling of VIFCC is complicated and time consuming. On the contrary the 2-D modeling is relatively simple and fast. Nevertheless, the application of 2-D modeling in the copper-crucible suffers the difficulty of asymmetry. The copper-crucible is not a solid but composed of slits among copper

segments. To overcome this difficulty in 2-D modeling, a method of superimposition of a layer of copper crucible and a slit of space was proposed to use in the simulation of the melting of VIFCC. The approach is based on the assumptions that there are axisymmetric system and quasi-steady state, besides the angle between the copper segment and slit of space is small so that they can be treated as near parallel as seen in Fig.3.

The cross section pass through line A-B which shows a layer of copper crucible part in Fig.2a is presented in Fig.4a, and the other cross section pass through line A-C in Fig.2b which shows a slit of space part is shown in Fig.4b. After computing these two parts, the results of two temperature distributions in a real volume ratio (slit space : copper crucible= 3 : 7) of VIFCC system are added to obtain the final temperature distribution.

In this study, a coupling between electromagnetic and thermal field has been applied to the ca lculation with sequential method, which is one choice of coupling provided in ANSYS software. It is possible to optimize the meshes of each physical field, according to their

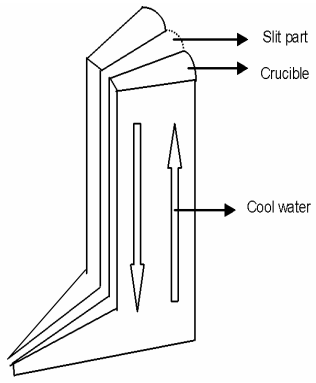

Fig.3 The drawing between the copper segment and slit of space.

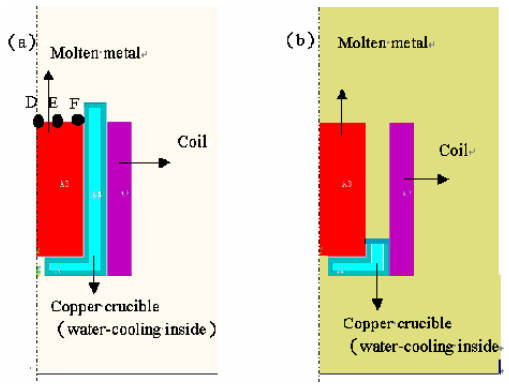

Fig.4 A cross-section along line A-B (a) and line A-C (b) in Fig.2.

influence on the problem. The resolution time base (with a step by step method) will be adapted for each kind of time constants which can be very different from one solution to another[8]. To overcome the different physical environment problems, we use a simple time route function to update our analysis of the sequence.Simulation starts with the analysis of magnetic field then substitute the joule heat generated by the eddy current into the governing equation of thermal field analysis and then the temperature is feed back to the choice of physical properties of magnetic analysis[9] as shown in Fig.5.

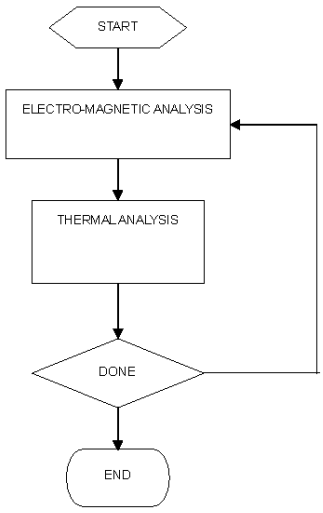

Fig.5 Flowchart of the simulation procedure.

In order to solve the changes of material properties with increase of time, a function has been derived with the data of table to update the property such as resistivity, conductivity (see Table 1), and permeability (H/m) is Al-0.002Ti 1.0002, copper 0.99999, air 1.00000. As to the problem of change of solid-liquid phase , the calculation has proposed a method of enthalpy with nonlinear data as shown in Table 2 to solve the difficulty. Since there is limited data for the property of Al-Ti alloy, an approximate Eq.(10) with the properties of

$$Y_{\mathrm{Al-Ti}} = X_{\mathrm{Al}} Y_{\mathrm{Al}} + X_{\mathrm{Ti}} Y_{\mathrm{Ti}} \tag{10}$$

Table 1 Magnetic resistivity and thermal conduction

Temperature	Al-0.002Ti		Cu	
℃	Resistivity, Ωm	Conduction, W/(m·℃)	Resistivity, Ωm	Conduction, W/(m·℃)
20	27.786	230.772	20 (25)	398
100	40.92	233.704	22 (77)	394
200	53.496	231.07	29 (127)	392
300	64.072	226.201	36 (227)	388
400	77.15	221.372	43	
500	92.42	205.851	50	
600	105.494	-	57	
700	117.171	-		

Table 2 Enthalpy of Al-0.002Ti and Cu

Temperature	Al-0.002Ti		Cu	
K	c_p^0, J/(mol·K)	Enthalpy, J/mol	c_p^0, J/(mol·K)	Enthalpy, J/mol
298.15	24.31142	0	24.45	0
400	25.6514	2548.938	25.43	2542.8
500	26.30218	5169.276	26.15	5123
600	26.38398	7899.392	26.74	7768.8
700	27.8929	10754.55	27.25	10469.9
800	29.25214	13756.41	27.71	13217.6
900	30.83096	16929.23	28.14	16011
933	32.66728	28804.71		
1000	31.74912	30924.56		

pure metals[10] is utilized to calculate the properties of alloys with the properties of pure metals in the simulation.

The boundary condition: In electromagnetic field analysis, the frequency of power supply in induction melting is 60kHz, and the current in each coil of the eight turns is 40A. In thermal field, the initial and ambient temperatures are chosen to be at 25℃ and water temperature at 60℃. The finite element mesh is shown in Fig.6, and the node numbers are 13640.

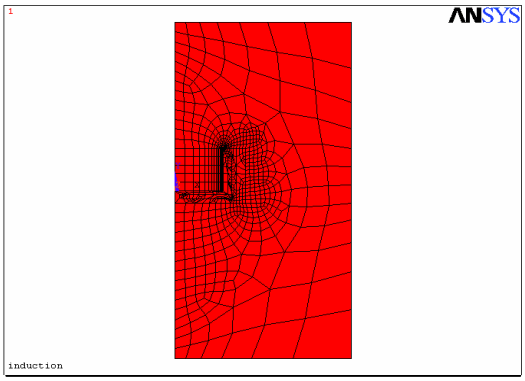

Fig.6 The finite element mesh.

3. VIFCC Experiment

One-kg of Al-0.2wt%Ti alloy is prepared in a vacuum induction furnace with cold-crucible of 3kg capacity to the melting experiments. The surface of the aluminum and titanium raw materials, were cleaned by acid and pre-heated. The VIFCC furnace is vacuumed to a base pressure of 1.3×10^{-2}Pa.

The induction power supply is 30kW max. The temperatures of the melt at D, E, F position (Fig.4a) were measured with a pyrometer. The cold copper crucible used has an inner radius of 50mm, an outer radius of 64mm, and a height of 125mm with 12 slots.

In order to understand the distribution of temperature and temperature gradient inside the ingot, an indirect method with solidified alloy macrostructures of the alloys melt was also applied.

The Al-Ti ingot was first cut in center-vertical direction. The cut-off section of the ingot was polished to finish with 0.5μm grade Al_2O_3 powder and etched by an etchant solution of HF : HCl : HNO_3 = 1 : 3 : 1 ratio by volume. The compositions of the raw material and ingot given in Table 3 are analyzed with electron probe microanalysts (EPMA).

Table 3 The chemical analysis of the raw material and ingot

Material	Al	Si	Fe	Cu	Mn	Mg	Cr	Zn	Ti	Ni	Pb
Raw	99.639	0.0667	0.187	0.0116	0.0138	0.0116	0.010	0.011	0.0155	0.015	0.0154
Ingot	99.581	0.0442	0.165	0.0002	0.0007	0.0000	0.000	0.000	0.2047	0.002	0.0015

4. Results and Discussion

In the present study, the validity of the whole model was examined with the surface temperature of the melt and the solidification structure. In order to verify our simulation, all the experimental variables are the same as the model.

4.1 Experimental results

Fig.7 shows the melted ingot of Al-0.02wt% Ti alloy. The macrostructure in the vertical cross-section of the ingot is shown in Fig.8. The macro-etched section of Al-Ti alloy is free from

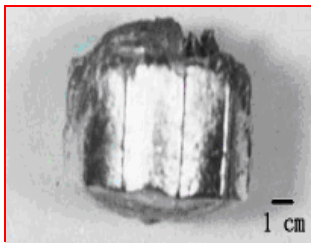

Fig.7 The Al-Ti ingot.

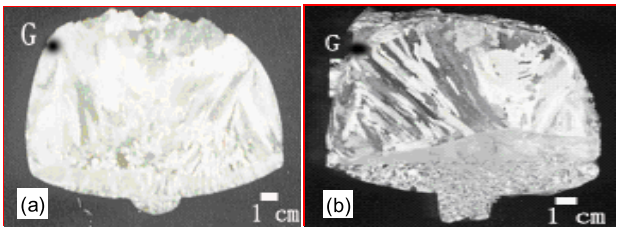

Fig.8 The solidification structures of the Al-Ti ingot: (a) dendrite structure; (b) directional structure.

porosity. Fig.8a shows the morphology of the dendrites, which grows outward from the center part to the G point contacting the crucible wall. Two symmetric triangular parts are observed in the corner section of the macrostructure. This might be due to the high temperature part as to form a mushy zone. However, the fine columnar crystals of dendritic structure developed perpendicularly on bottom surfaces (contact the copper-crucible). After controlling the cooling rate and the volume of the alloy, we obtain a nearly directional structure as shown in Fig.8b. The ingot exhibited most columnar grains, aligned almost parallel to the vertical axis in the middle section. By judging from the solidification structure, the solid-liquid interface has the shape of upward convex progressively and the crystals mainly grow outwards. The findings suggest the possibility of producing a single crystal by inducing preferential growth of a crystal whose growth direction coincides with the direction of heat flow distribution in VIFCC process.

4.2 Simulation results

A briefly description of the new superimposition method of a layer of copper and a slit is explained in the next paragraphs. The new superimposition method of a layer of copper and a slit is established.

First the calculation of temperature distribution was carried out with only a layer of copper crucible, and the results are shown in Fig.9. Fig.10 shows the relationship between temperature and time in different positions of the melting surface as in Fig.4. It can be seen in Fig.9, that only the portion of alloy over 640℃ is melted, which is less than the actual melted portion shown in Fig.8. The calculated temperatures are lower than those measured values from the actual molten metal as in Fig.10. It is obvious that the slit section in the simulation model plays an important role of VIFCC model. Another calculation under the same physical conditions was carried out with the only space of slit section and the result was shown in Fig.11. Without heat loss and induced current in copper crucible, it is observed that the highest temperature on the surface is in the position near to the coil as shown in

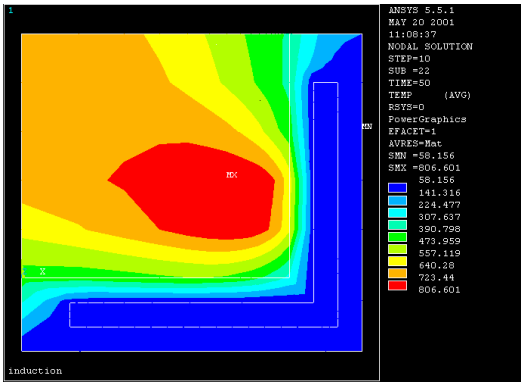

Fig.9 The final temperature (℃) distribution with the distance (mm) from ingot centerline after 50min melting.

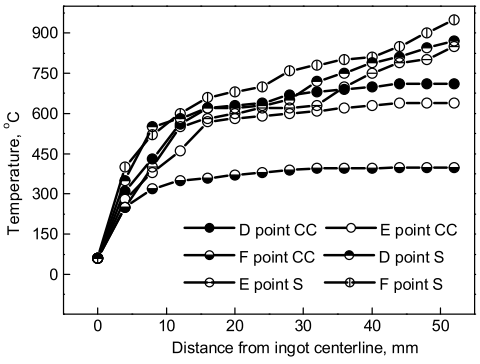

Fig.10 The relationship between temperature and time in different locations of the melting surface (CC means calculation with copper-crucible, and S means at the slit part).

Figs. 9 and 11. Furthermore, the temperature distribution is higher and uniform than the one calculated with only a single copper layer as shown in Fig.9. It is evident that the slit can allow more electromagnetic flux flown into the melts. However, inferring from the actual macrostructure of solidified ingot and measured surface temperatures, the molten parts are different from the results of Figs. 9 and 11 and the measured surface temperature are different from those of Figs. 10 and 12.

An improvement has been made by introducing the ideal of superimposition of layer of a copper crucible and a slit of space and the result is presented in Fig.13. The isothermal line of Fig.13 is made up of averaging the values of temperatures from two added layers (overlay the crucible : with the slot) with a weight ratio of 7 : 3. The corrected Fig.12 shows the molten parts of Al-Ti alloys are closer to the real molten parts in Fig.7 and it indicates that the temperature gradient actually exists in the molten metal which causes different dendrite and fine grain structures. A comparison between simulation and experimentally measured data for this system are given in Figure 11, the error is less than 3%. The newly predicted method is reasonably close to the experimental one.

It can also be demonstrated by the solidification structure, with proper controlling of melting in VIFCC system, a near directional solidification dendrite grains could be obtained as discussed before. The macro-structure could qualitatively give details of the temperature distribution in the ingot.

This simple proposed analysis presented fairly satisfactory results between the calculated temperature distribution and the real macro-etched solidified structures.

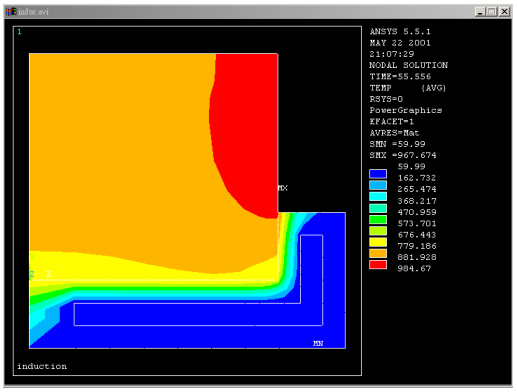

Fig.11 The final temperature (℃) distribution with the distance (mm) from ingot centerline in the model with the slit section.

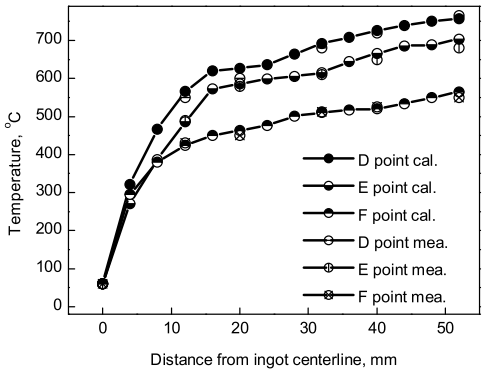

Fig.12 The temperature comparison. The symbol "cal." means the calculated result by 70% with copper-crucible and 30% with slit part. The symbol "mea." means the measurement.

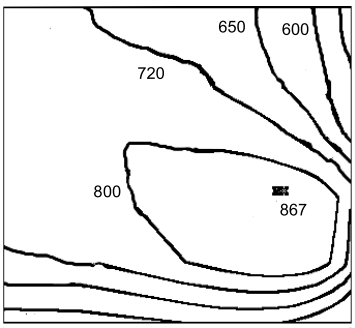

Fig.13 The isothermal final temperature (℃) line calculation based on 30% with slit + 70% crucible with the distance (mm) from ingot centerline.

5. Conclusions

In this paper, a simple modified 2-D model was proposed to simulate the melting process in VIFCC.

The simulation results are compared with experimental data both in temperature measurement and macrostructure. They show a good agreement with each other. Although the VIFCC procedure has advantage in melting high purity metals or alloys, the non-uniform temperature distribution prevails in the molten alloy. This may lead to the non-uniform composition and grain size. Even though there is congenital deficiency, we obtained a nearly directional solidification structure by controlling the experimental variables with the aid of simulated computation. So the technique developed in this study can be helpful to make proper design and operation in the melting process. Furthermore we can have an optimal property for the target material by VIFCC process.

It could be demonstrated that the simple 2-D model with superimposition of a layer of copper and a slit to simulate the melting process in VIFCC is feasible.

REFERENCES

1 D.J. Chronister, S.W. Scott, D.R. Stickle, D. Eylon and F.H. Froes, *Journal of Metals* **(9)** (1986) 51.
2 G.H. Schippereit, A.F. Leatherman and D. Evers, *Journal of Metals* **(2)** (1961) 140.
3 K. Sakamoto, K. Yoshikawa, T. Kusamichi and T. Onoye, *ISIJ International* **32(5)** (1992) 616.
4 H. Tsuboi, M. tanaka, F. Kobayashi and T. Misaki, *IEEE Transactions on Magnetics* **29(2)** (1993) 1574.
5 T. Morisue, T. Yajima, T. Kume and S. Fujimori, *IEEE Transactions on Magnetics* **29(2)** (1993) 1562.
6 C. Chaboudez, S. Clain, R. Glardon, D. Mari, J. Rappaz and M. Swierkosz, *IEEE Transactions on Magnetics,* **33(1)** (1997) 739.
7 K. Sadeghippour, J.A. Dopkin and K. Li, *Computers in Industry* **28** (1995) 195.
8 P. Eustache, G. Meunier and J.L. coulomb, *Transactions on Magnetics* **32(3)**(1996) 1461.
9 ANSYS 5.5 Program Langrage On-Line Help, http://www.ansys.com/.
10 Metals Handbook Vol.2: Properties and Selection: Nonferrous Alloys and Special-Purpose Materials, (Tenth ed., ASM International, 1990) p.152, 346.

Appendix 1 List of symbles

Symble	Nomenclature
$\nabla\times$	Curl operator
$\nabla\cdot$	Divergence operator
H	Magnetic field intensity vector
$\{\boldsymbol{J}\}$	Total current density vector
$\{\boldsymbol{J}_{\mathrm{s}}\}$	Applied source current density vector
$\{\boldsymbol{J}_{\mathrm{e}}\}$	Induced eddy current density vector
$\{\boldsymbol{D}\}$	Displacement vector
t	Time
$\{\boldsymbol{E}\}$	Electric field intensity vector
$\{\boldsymbol{B}\}$	Magnetic flux density vector
ρ	Electric charge density
$[\mu]$	Magnetic permeability matrix, in general a function of $\{\boldsymbol{H}\}$
$[\sigma]$	Electrical conductivity matrix
T	Temperature
k	The thermal conductivity
c_p	The specific heat